Systems & Control Transactions

Research Article - Peer Reviewed Conference Proceeding
ESCAPE 35 - European Symposium on Computer Aided Process Engineering
Ghent, Belgium. 6-9 July 2025
Jan F.M. Van Impe, Grégoire Léonard, Satyajeet S. Bhonsale, Monika E. Polańska, Filip Logist (Eds.)

PSE PRESS

Solar Desalination and Porphyrin Mediated Visible-Light Photocatalysis in Decolouration of Dyes as Biological Analogues Applied in Advanced Water Treatment

Evans M. N. Chirwa*, Bezza F. Andualem, Osemeikhain Ogbeifun, Shepherd M. Tichapondwa, Wesley Lawrence and Bonhle Manoto

University of Pretoria, Department of Chemical Engineering, Pretoria, Gauteng, South Africa
* Corresponding Author: evans.chirwa@up.ac.za

ABSTRACT

Engineering can be made simple and more impactful by observing and understanding how organisms in nature solve eminent problems. For example, scientists around the world have observed green plants thriving without organic food inputs using the complex photosynthesis process to kick-start a self-sustaining biochemical food chain. In this study, two biological analogues for advanced water treatment, i.e., visible-light photocatalysis using porphyrin-$Bi_{12}O_{17}Cl_2$ and $BiOIO_3$ compounds and interfacial solar desalination by a by Reduced Graphene Oxide-Black TiO_2 (rGO-Black TiO_2) were investigated. For the visible-light photocatalytic process for dye decolouration, a porphyrin@$Bi_{12}O_{17}Cl_2$ system was applied to successfully degrade Rhodamine B dye in batch experiments, achieving up to 79% degradation within 240 minutes. These results show that more advances and more efficient engineered systems can be achieved by observing nature and how these systems have survived over billions of years. The rGO-Black TiO_2 system achieved increases in temperature for 25oC to 60oC in less than 5 seconds. Based on these observations, the research group from the Water Utilisation Group at the University of Pretoria have studied and developed fundamental processes for the degradation and remediation of unwanted compounds such as disinfection byproducts (DBPs), volatile organic compounds (VOCs) and pharmaceutical products from water.

Keywords: solar desalination, heterogenous photocatalysis, 3D-printed Graphene Oxide, advanced water treatment, biological analogues.

INTRODUCTION

Desalination

The crucial demand for sustainable and eco-friendly desalination technologies propelled by renewable energy is essential for overcoming global water scarcity. Solar desalination has been recognised as a prominent technology as it exploits solar energy to produce clean water through sufficient thermal management and the localisation of heat using a solar absorber [1].

Currently, Reverse osmosis (RO) is the most broadly used process for saline water treatment, as well as industrial and drinking water. Roughly 53 % of the feed water for RO systems is seawater followed by mostly brine, fresh water, and treated wastewater. The multi-stage flash (MSF) and multi-effect distillation (MED) are the second and third most used technologies, respectively. Reverse osmosis, MED and MSF technologies constitute 94 % of the overall desalinated water produced. Solar-powered desalination via photovoltaic desalination and solar thermal evaporation constitute less than 1 %. Of the global freshwater desalinated, membrane-based processes account for 71 % of the total capacity produced and thermal processes make up the other 29 %. This displays the historical mass application of membrane-based desalination technologies. The advantage of utilising seawater RO or brackish water RO is due to the total energy costs of seawater RO (3 – 4 kWh·m-3) and brackish water RO (0.5 – 2.5 kWh·m-3) desalination being lower than the energy required for thermal desalination technologies such as MSF (14 – 25.5 kWh·m-3) and MED (6.5 – 11 kWh·m-3) which requires the use of electrical and thermal energy. The energy cost difference between seawater RO and brackish water RO is due to brackish water having a substantially lower osmotic pressure compared to seawater and thus requiring less energy. The high salinity concentration of seawater limits the osmosis process due to affecting the osmosis pressure, requiring more energy. However, the economic cost of seawater desalination using MSF or MED is proportionate to that of RO as a result of the lower investment costs. The availability and cost of energy account for more than 30 % of the total desalination cost. It is estimated that the present global desalination capacity roughly consumes a minimum of 75.2 TWh annually, which is equivalent to 0.4 % of the global electricity usage.

Solar-driven absorbers generally involve a mono or bi-layer design, comprising a solar-light absorber and a floating substrate. The solar absorber converts incident light into heat energy, while the floating substrate facilitates water transfer to the active vapour generation site and minimising heat energy loss through conduction [2].

The ongoing challenge of salt accumulation on the surface of the solar absorber as a result of the high salt concentration in the bulk water body leads to the obstruction of light absorption, subsequently hindering freshwater vapour release and efficient photothermal efficiency [1].

Recent research motivated by the modification of natural saline inhabiting vegetation (halophyte plants) has been employed to embrace the biomimetic principle for numerous engineering practices such as freshwater steam generation and salt rejection [3] Naturally, plants possess inherent capabilities which harness solar energy and groundwater in the photosynthesis process to create oxygen and carbohydrates. For example, trees make use of their trunk and leaves for continuous nutrient and water transfer for nourishment. This principle has inspired wood-based solar absorbers for solar steam generation. For example, carbon nanotube-modified flexible wood membranes [4] and graphite-coated wood solar absorbers [5] have demonstrated great potential.

Sun *et al.* proposed a three-dimensional (3D) solar evaporator inspired by the outer shell structure of Vasticardium vertebratum, demonstrating a 95% evaporation efficiency and a superb evaporation rate of 1.73 kg/m^2·h while effectively preventing salt accumulation [3]. Furthermore, mangrove-inspired configurations [6] provide promising potential aimed at bio-mimicking solar absorbers. This is driven by the inherent water transfer and salt-tolerant characteristics of mangrove trees which regulate water and ion absorption [6]. Solar absorbers utilising a graphene oxide-reduced graphene oxide (GO-rGO) lotus leaf-inspired Janus film [7] or mangrove-mimicked designs have displayed efficient photothermal conversion performance and high evaporation rates of seawater [8].

Black titanium dioxide (TiO_2) has the ability to absorb immense ultraviolet-visible (UV-Vis) light for chemical or electrical energy conversion owing to the enhanced photocatalytic performance from the introduction of lattice disorder. Black TiO_2 can be obtained by establishing oxygen vacancies and Ti^{3+} doping into the TiO_2 lattice using chemical reduction [9]. The combination of carbon-based materials such as GO with TiO_2 has displayed a synergistic effect between the two constituents as the photoactive TiO_2 integrates with the adsorption potential imparted by carbon. Carbon can assist in charge separation and obstruct electron-hole recombination in TiO_2 [10] .

The bio-inspired structural fabrication of rGO was designed for water and heat transfer abilities similar to that of plant root cells. Black TiO_2 can be utilised to minimise light reflection and efficiently absorb light across the UV-near infrared region, inspired by black snake scales.

Photocatalysis

Recently, photocatalysis has garnered attention for pollution mitigation. The technology is amenable to visible light activation which make up 42%–43% of the solar spectrum [11]. To cut down on greenhouse gases emission, the leaning towards solar-driven processes is unavoidable. Solar energy is renewable and abundant.

In Photocatalytic process semiconductor photocatalyst, materials are activated by sufficient photon to generate electrons (e^-) and holes (h^+) [12]. The e^- and h^+ in subsequent reaction with dissolved O_2 and H_2O produce superoxide anion radicals ($\bullet O_2^-$) and hydroxyl radicals (.OH), with the ability to destroy adsorbed pollutant on the photocatalyst [13-15].

Generation of abundant e^- and h^+, separation and boosting redox ability is crucial for material performance. These have been achieved via plasmon resonance effect [16]heterojunction formation [17], ion doping [18], photosensitization effect [19] and other strategies. In photosensitization strategy light sensitive or absorbing material such as porphyrin are apply to photocatalyst enhance visible light utilization [20], and ultimately the photocatalytic ability of photocatalyst.

Porphyrins are organic molecules are similar to the structure of chlorophyll in plant. They are efficient absorber of visible light, producing a photochemical reaction [21]. Porphyrin can be modified into different shapes sucha s rods, hexagonal, hollow spheres, tubes [22]. The complexity of versatility of in terms of assembly of the molecules make them useful in various application including photocatalysis. Porphyrin have been combined with graphite carbon nitrides [23]; Fe_3O_4 [24]; TiO_2 [25], BiOCl [26], ZnO nanofiber composite [27], graphene [28] and $Bi_{12}O_{17}Cl_2$ [29], where they demonstrated enhanced photodegradation in comparison with individual porphyrin and the inorganic photocatalyst components.

Solar desalination is viewed as one of the most sustainable ways of dealing with the global energy challenge with emerging technological advancements. The technology is highly efficient in that the solar energy is targeted at the interface between a water surface and solar absorbing material to achieve evaporation with minimal energy losses. In addition, notable innovations can be found in adsorption desalination and energy-efficient freeze desalination. The work outlined here has been patented by several leading researchers around the world but no full-scale plant has not yet been built to demonstrate the economic feasibility of this technology at the date of publication of this article.

APPLICATIONS AND PERFORMANCES OF MATERIALS

Performance of TiO_2/rGO in Desalination

Excellent solar absorption potential across the UV-Vis solar spectrum for solar absorbers is crucial for achieving efficient desalination [30]. As presented in Figure 1, the black TiO_2/rGO composite exhibited remarkable light absorption potential across the ensure UV-Vis region in comparison to white TiO_2 which displayed good UV light absorption with almost no visible light absorption and rGO showed excellent visible light absorption, however, the light absorption across the UV spectrum was similar to that of white TiO_2. Therefore, demonstrating the enhanced light absorption performance of the composite where the beneficial attributes of each component act synergistically.

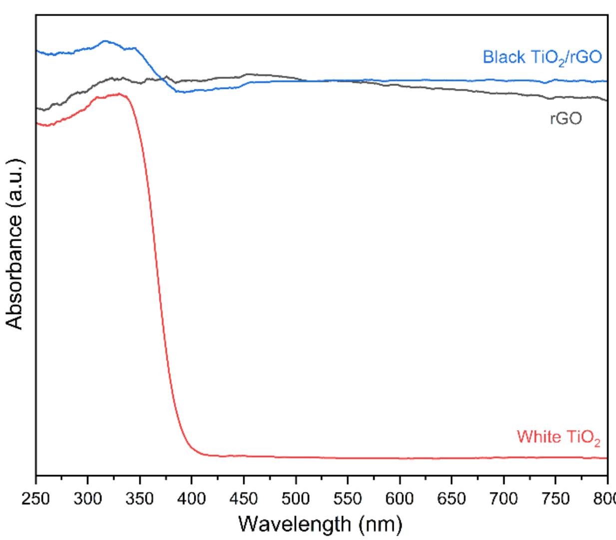

Figure 1. UV-Vis DRS spectra of rGO, white TiO_2, and black TiO_2/rGO.

In solar-driven desalination, the water evaporation rate can be determined using [31].

$$v = \frac{\Delta m}{A \times t} \quad (1)$$

Where v is the evaporation rate (kg/m^2·h), Δm is the change in mass due to water evaporation (kg), A represents the evaporation area (m^2), and t is the duration of the evaporation process (h). The photothermal conversion or steam generation efficiency, η, can be determined using [5] :

$$\eta = \frac{v \cdot H_{LV}}{P} \quad (2)$$

$$H_{LV} = h_v + C\Delta T \quad (3)$$

Where H_{LV} is the total liquid-vapour phase change enthalpy, P is the solar power density (1 kW/m^2), h_v represents the latent heat of vaporisation (kJ/kg), C is the specific heat capacity of water (4.2 kJ/kg·K), and ΔT is the temperature increase of water (K). The freshwater vapour generation (Figure 2b) was determined to be 1.19 kg/m^2·h with an 82.38% photothermal conversion efficiency. The solar absorber displayed a surface temperature increase of 23.8°C (Figure 2a) within 120 min of commencing the desalination test. Furthermore, the bio-inspired solar absorber demonstrated effective salt rejection of the surface owing to the small interlayer spacings and the negatively charged surface of the rGO nanopores.

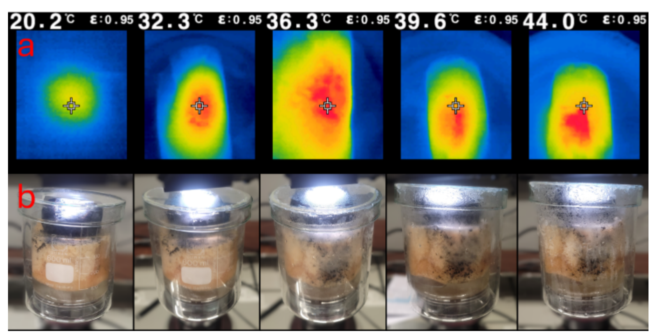

Figure 2. IR thermal images of the black TiO_2/rGO solar absorber (a) and photos of the solar desalination test (b) taken every 30 min.

Performance of Porphyrin/$Bi_{12}O_{17}Cl_2$ in Pollutant Degradation

Tetrakis (4-carboxyphenyl) porphyrin (TCPP), a member of porphyrin, coupling with $Bi_{12}O_{17}Cl_2$ improved its performance. First, TCPP was modified to a rod shape and applied to $Bi_{12}O_{17}Cl_2$ to form composites.

The degradation study was carried out using Rhodamine as a model pollutant. The experiment involved a simple batch degradation study in a beaker, where TCPP-Bi12O17Cl2 composite was dispersed in the solution of Rhodamine dyes. The reaction was sufficiently stirred in the dark to achieve absorption-desorption equilibrium. Thereafter, it was irradiated with visible light to initiate the photocatalytic degradation of the dye. The result of dye degradation overtime on the materials 0.02%wtTCPP-$Bi_{12}O_{17}Cl_2$,0.4%wtTCPP-$Bi_{12}O_{17}Cl_2$ 1%wtTCPP-$Bi_{12}O_{17}Cl_2$, $Bi_{12}O_{17}Cl_2$, TCPP are presented in Figure 3. Within 240 min, the 52%, 68%, 79%, 40% and 20% degradation were achieved.

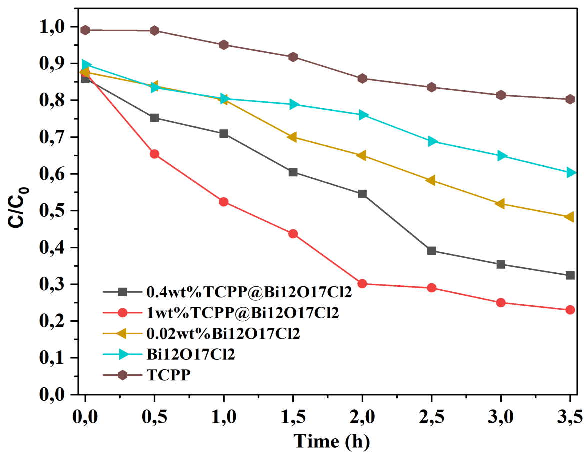

Figure 3. Photocatlytic decolourization of Rhodamine B dye

The performance of the TCPP/$Bi_{12}O_{17}Cl_2$ was attributed to the expanded visible light response and composite/heterojunction formation. Figure 4(a) shows the shift of the absorption edge of pristine $Bi_{12}O_{17}Cl_2$ with the introduction of TCPP. The enhanced visible light response favoured increased electrons and hole generation from the sufficient capture of the visible light by the porphyrin molecules. Figure 4(b) shows the material's Electrochemical impedance spectroscopy (EIS). Data from EIS provide transport and separation of electrons and holes. A smaller semi-circle observed with TCPP-load $Bi_{12}O_{17}Cl_2$ indicates superior transport and separation of the photogenerated electron and hole, the reason for the strengthened photodegradation activity of the dye.

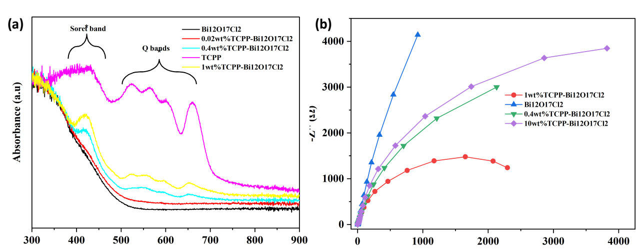

Figure 4. UV vis DRS (a) and EIS spectra of material (b)

When porphyrin-$Bi_{12}O_{17}Cl_2$ is exposed to visible light, electrons are excited from the highest occupied molecular orbital (HOMO) to the lowest unoccupied molecular orbital (LUMO) [32]. These excited electrons in the LUMO are subsequently transferred to the conduction band (CB) of the host material [25], effectively separating them from the corresponding holes [33]. This separation enhances the photocatalytic efficiency of the system.

CONCLUSION AND FUTURE WORK

In summary, the bioinspired 3D black TiO_2/rGO solar absorber demonstrated efficient freshwater evaporation and photothermal conversion efficiency. This can be attributed to the successful mimicking of plant root cells for water transfer and the light absorption ability of black snake scales. These results show the promising potential for further advancing bioinspired photothermal solar absorbers.

Also, using porphyrin, a biological analogue of chlorophyll, proved advantageous for visible light capture in the porphyrin-$Bi_{12}O_{17}Cl_2$ system for pollutant degradation.

This work reported on one example of the porphyrin-$Bi_xO_yX_z$ system, TCPP-$Bi_{12}O_{17}Cl_2$. The porphyrin-BixOyXz system is diverse considering the many forms of porphyrin structures and morphologies available, as well as $Bi_xO_yX_z$. Further exploration of the combinations, therefore, in the system holds potential in photocatalysis. Porphyrin-BiOIO3 is also proposed, where the visible light absorption of $BiOIO_3$ enhancement is envisaged. Comparatively, $BiOIO_3$ has good electron and hole separation upon activation. However, it cannot be activated due to the wide gap energy, hence the proposed composite with porphyrin.

ACKNOWLEDGEMENTS

The study was funded by the National Research Foundation (NRF) through Grant No's. SRUG2204072544 and EQP180503325881 and Rand Water Company, through Grant No. RW01413/18 awarded to Prof E.M.N. Chirwa, and The NRF Thuthuka Fund Grant No. TTK18024324064 awarded to Prof S.M. Tichapondwa at the University of Pretoria

REFERENCES

1. Wu L, Dong Z, Cai Z, Ganapathy T, Fang NX, Li C, Yu C, Zhang Y, Song Y, 2020. Highly efficient three-dimensional solar evaporator for high salinity desalination by localized crystallization. *Nature Communications*. 11:521. 10.1038/s41467-020-14366-1 (2020)
2. Dai X, Guan H, Wang X, Wu M, Jiang P, Chai Y, Wang X, 2024. Apple leaf-inspired bilayered Janus wood evaporator with decoupled light-vapor interfaces for high-efficiency solar steam generation. *Chem Eng J*. 499:155796.

https://doi.org/10.1016/j.cej.2024.155796 (2024)

3. Sun S, Shi C, Kuang Y, Li M, Li S, Chan H, Zhang S, Chen G, Nilghaz A, Cao R, Tian J, 2022. 3D-printed solar evaporator with seashell ornamentation-inspired structure for zero liquid discharge desalination. *Water Res.* 226:119279. https://doi.org/10.1016/j.watres.2022.119279 (2022)
4. Liu H, Chen C, Chen G, Kuang Y, Zhao X, Song J, Jia C, Xu X, Hitz E, Xie H, Wang S, Jiang F, Li T, Li Y, Gong A, Yang R, Das S, Hu L, 2018. High-Performance Solar Steam Device with Layered Channels: Artificial Tree with a Reversed Design. *Advanced Energy Materials.* 8:1701616. https://doi.org/10.1002/aenm.201701616 (2018)
5. Li T, Liu H, Zhao X, Chen G, Dai J, Pastel G, Jia C, Chen C, Hitz E, Siddhartha D, Yang R, Hu L, 2018. Scalable and Highly Efficient Mesoporous Wood-Based Solar Steam Generation Device: Localized Heat, Rapid Water Transport. *Adv Funct Mater.* 28:1707134. https://doi.org/10.1002/adfm.201707134 (2018)
6. Wang Y, Lee J, Werber JR, Elimelech M, 2020. Capillary-driven desalination in a synthetic mangrove. *Science Advances.* 6:eaax5253. doi:10.1126/sciadv.aax5253 (2020)
7. Han D-D, Chen Z-D, Li J-C, Mao J-W, Jiao Z-Z, Wang W, Zhang W, Zhang Y-L, Sun H-B, 2020. Airflow Enhanced Solar Evaporation Based on Janus Graphene Membranes with Stable Interfacial Floatability. *ACS Applied Materials & Interfaces.* 12:25435-25443. 10.1021/acsami.0c05401 (2020)
8. Abdelsalam MA, Sajjad M, Raza A, AlMarzooqi F, Zhang T, 2024. Sustainable biomimetic solar distillation with edge crystallization for passive salt collection and zero brine discharge. *Nature Communications.* 15:874. 10.1038/s41467-024-45108-2 (2024)
9. Tudu BK, Gupta V, Kumar A, Sinhamahapatra A, 2020. Freshwater production via efficient oil-water separation and solar-assisted water evaporation using black titanium oxide nanoparticles. *J Colloid Interface Sci.* 566:183-193. https://doi.org/10.1016/j.jcis.2020.01.079 (2020)
10. Ghumro SS, Lal B, Pirzada T, Qazi MA, Ali A, Altaf AA, Thebo KH, Kazi M, 2025. Exploring the hetero-catalytic proficiencies of pristine and carbon-doped titania nanocatalysts in dye degradation and their synergetic profiles against bacteria. *J Mol Struct.* 1319:139462. https://doi.org/10.1016/j.molstruc.2024.139462 (2025)
11. Hassaan MA, El-Nemr MA, Elkatory MR, Ragab S, Niculescu V-C, El Nemr A, 2023. Principles of Photocatalysts and Their Different Applications: A Review. *Top Curr Chem.* 381:31. 10.1007/s41061-023-00444-7 (2023)
12. Khan K, Tareen AK, Aslam M, Sagar RUR, Zhang B, Huang W, Mahmood A, Mahmood N, Khan K, Zhang H, Guo Z, 2020. Recent Progress, Challenges, and Prospects in Two-Dimensional Photo-Catalyst Materials and Environmental Remediation. *Nano-Micro Letters.* 12:167. 10.1007/s40820-020-00504-3 (2020)
13. Arumugam M, Choi MY, 2020. Recent progress on bismuth oxyiodide (BiOI) photocatalyst for environmental remediation. *Journal of Industrial and Engineering Chemistry.* 81:237-268. https://doi.org/10.1016/j.jiec.2019.09.013 (2020)
14. Wang Y, Shi Z-q, Fan C-m, Hao X-g, Ding G-y, Wang Y-f, 2012. Synthesis of BiOCl photocatalyst by a low-cost, simple hydrolytic technique and its excellent photocatalytic activity. *International Journal of Minerals, Metallurgy, and Materials.* 19:467-472. 10.1007/s12613-012-0581-7 (2012)
15. Lal M, Sharma P, Singh L, Ram C, 2023. Photocatalytic degradation of hazardous Rhodamine B dye using sol-gel mediated ultrasonic hydrothermal synthesized of ZnO nanoparticles. *Results in Engineering.* 17:100890. https://doi.org/10.1016/j.rineng.2023.100890 (2023)
16. Zhang M, Bi C, Lin H, Cao J, Chen S, 2017. Construction of novel Au/Bi12O17Cl2 composite with intensive visible light activity enhancement for contaminants removal. *Mater Lett.* 191:132-135. https://doi.org/10.1016/j.matlet.2016.12.089 (2017)
17. Bi C, Cao J, Lin H, Wang Y, Chen S, 2016. BiOI/Bi12O17Cl2: A novel heterojunction composite with outstanding photocatalytic and photoelectric performances. *Mater Lett.* 166:267-270. https://doi.org/10.1016/j.matlet.2015.12.089 (2016)
18. Yang Y, Zeng Y, Jin T, Zhang X, Teng H, Wang S, Chen H, 2022. Construction of oxygen vacancy on Bi12O17Cl2 nanosheets by heat-treatment in H2O vapor for photocatalytic NO oxidation. *Journal of Materials Science & Technology.* 123:234-242. https://doi.org/10.1016/j.jmst.2022.02.018 (2022)
19. Ye L, Su Y, Jin X, Xie H, Zhang C, 2014. Recent advances in BiOX (X = Cl, Br and I) photocatalysts: synthesis, modification, facet effects and mechanisms. *Environmental Science: Nano.* 1:90-112. 10.1039/C3EN00098B (2014)
20. Zheng H, Chen G, Zhang A, Tan Z, Wang R, Wang H, Mei Y, Zhang X, Ran J, 2021. Enhanced photocatalytic activity of Bi24O31Br10 microsheets constructing heterojunction with AgI for Hg0 removal. *Sep Purif Technol.* 262:118296. https://doi.org/10.1016/j.seppur.2020.118296 (2021)

21. Joseph M, Haridas S, 2020. Recent progresses in porphyrin assisted hydrogen evolution. *Int J Hydrogen Energy.* 45:11954-11975. https://doi.org/10.1016/j.ijhydene.2020.02.103 (2020)
22. Medforth CJ, Wang Z, Martin KE, Song Y, Jacobsen JL, Shelnutt JA, 2009. Self-assembled porphyrin nanostructures. *Chem Commun.* 7261-7277. 10.1039/B914432C (2009)
23. Mei S, Gao J, Zhang Y, Yang J, Wu Y, Wang X, Zhao R, Zhai X, Hao C, Li R, Yan J, 2017. Enhanced visible light photocatalytic hydrogen evolution over porphyrin hybridized graphitic carbon nitride. *J Colloid Interface Sci.* 506:58-65. https://doi.org/10.1016/j.jcis.2017.07.030 (2017)
24. Rabbani M, Rafiee F, Ghafuri H, Rahimi R, 2016. Synthesis of Fe3O4 nonoparticles via a fast and facile mechanochemicl method: Modification of surface with porphyrin and photocatalytic study. *Mater Lett.* 166:247-250. https://doi.org/10.1016/j.matlet.2015.12.087 (2016)
25. Wang H, Zhou D, Wu Z, Wan J, Zheng X, Yu L, Phillips DL, 2014. The visible light degradation activity and the photocatalytic mechanism of tetra(4-carboxyphenyl) porphyrin sensitized TiO2. *Mater Res Bull.* 57:311-319. https://doi.org/10.1016/j.materresbull.2014.06.017 (2014)
26. Zhao P, Huang Y, Chen J, Shao S, Miao H, Xia J, Jia C, Hua M, 2020. Preparation of meso-tetraphenyl porphyrin modified defect-rich BiOCl with enhanced visible-light photocatalytic activity for antibiotic degradation and mechanism insight. *Journal of Photochemistry and Photobiology.* 3-4:100014. https://doi.org/10.1016/j.jpap.2020.100014 (2020)
27. Vo HT, Nguyen AT, Tran CV, Nguyen SX, Tung NT, Pham DT, Nguyen DD, La DD, 2021. Self-Assembly of Porphyrin Nanofibers on ZnO Nanoparticles for the Enhanced Photocatalytic Performance for Organic Dye Degradation. *ACS Omega.* 6:23203-23210. 10.1021/acsomega.1c02808 (2021)
28. La DD, Rananaware A, Salimimarand M, Bhosale SV, 2016. Well–dispersed assembled porphyrin nanorods on graphene for the enhanced photocatalytic performance. *ChemistrySelect.* 1:4430-4434. https://doi.org/10.1002/slct.201601001 (2016)
29. Ogbeifun O, Tichapondwa SM, Chirwa EMN, 2023. Self-assembled micro and nano rod-shaped porphyrin@Bi12O17Cl2 composite as an efficient photocatalyst for degradation of organic contaminants. *Discover Nano.* 18:137. 10.1186/s11671-023-03915-4 (2023)
30. Bezza FA, Iwarere SA, Brink HG, Chirwa EMN, 2024. Design and fabrication of porous three-dimensional Ag-doped reduced graphene oxide (3D Ag@rGO) composite for interfacial solar desalination. *Scientific Reports.* 14:13793. 10.1038/s41598-024-62987-z (2024)
31. Liu X, Zhu Q, Qian Y, Wu W, 2025. Enhanced photothermal interface evaporation via coupling of Ag-GO aerogel with thermal insulation substrate. *Sep Purif Technol.* 360:131080. https://doi.org/10.1016/j.seppur.2024.131080 (2025)
32. Moshari M, Rabbani M, Rahimi R, 2016. Synthesis of TCPP–Fe3O4@S/RGO and its application for purification of water. *Res Chem Intermed.* 42:5441-5455. 10.1007/s11164-015-2378-6 (2016)
33. Zhang Z, Liu H, Xu J, Zeng H, 2017. CuTCPP/BiPO4 composite with enhanced visible light absorption and charge separation. *Journal of Photochemistry and Photobiology A: Chemistry.* 336:25-31. https://doi.org/10.1016/j.jphotochem.2016.12.020 (2017)